High-Density Three-Dimension Graphene Macroscopic Objects for High-Capacity Removal of Heavy Metal Ions

Weiwei Li[1,2], Song Gao[1], Liqiong Wu[1], Shengqiang Qiu[1], Yufen Guo[1.2], Xiumei Geng[1], Mingliang Chen[1], Shutian Liao[1], Chao Zhu[1], Youpin Gong[1], Mingsheng Long[1], Jianbao Xu[1,2], Xiangfei Wei[1], Mengtao Sun[3] & Liwei Liu[1]*

[1]Key Laboratory of Nanodevices and Applications, Suzhou Institute of Nano-Tech and Nano-Bionics, Chinese Academy of Sciences, Suzhou, Jiangsu 215123, People's Republic of China.

[2]University of Chinese Academy of Sciences, 19A Yuquan Road, Beijing, 100049, People's Republic of China.

[3]Institute of Physics, Chinese Academy of Sciences, Beijing 100190, People's Republic of China.

[*]e-mail: lwliu2007@sinano.ac.cn

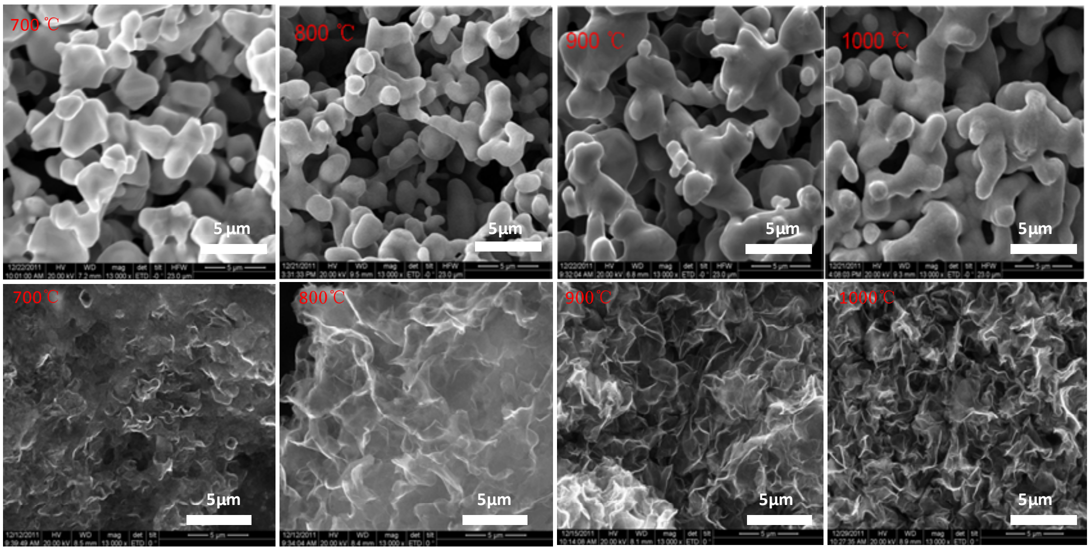

Supplementary Figure S1 | SEM images of the 3D-GMOs grown at different temperatures. Ni skeletons are removed (down) and not removed (up). The Ni particles are prone to cross-link and the quality of 3D-GMOs is gradually improved with increasing the growth temperature. When the growth temperature is lower to 700 °C, the SEM image shows that there is dominantly amorphous carbon, which is consisting with the Raman spectrum grown at 700 °C.

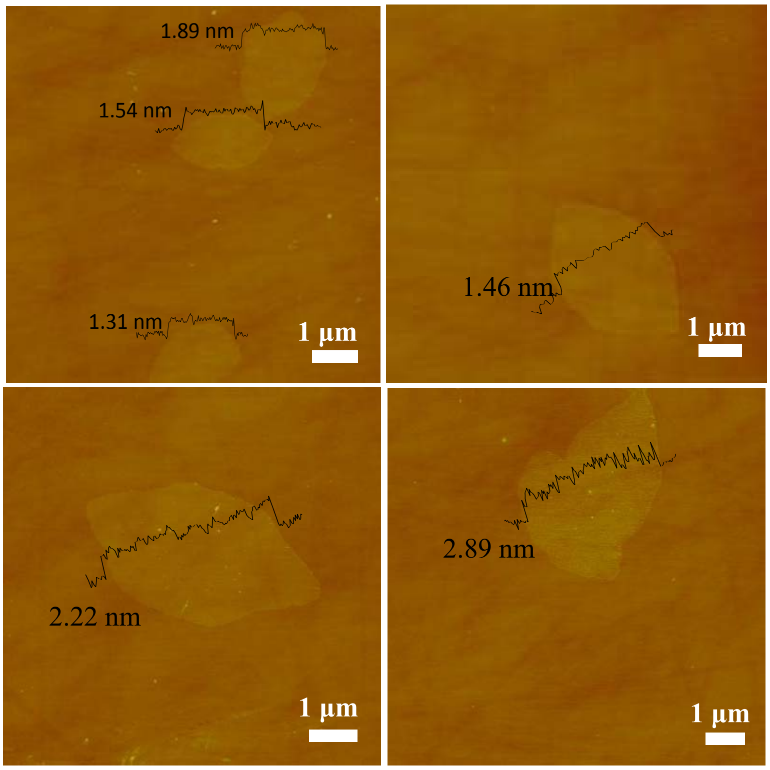

Supplementary Figure S2 | AFM images of the graphene layers of a 3D-GMO. AFM images show the height profile of the surface morphology of the graphene layers, and the step height are less than 3 nm, corresponding to the dominated range of graphene layer numbers of 1-7 L.

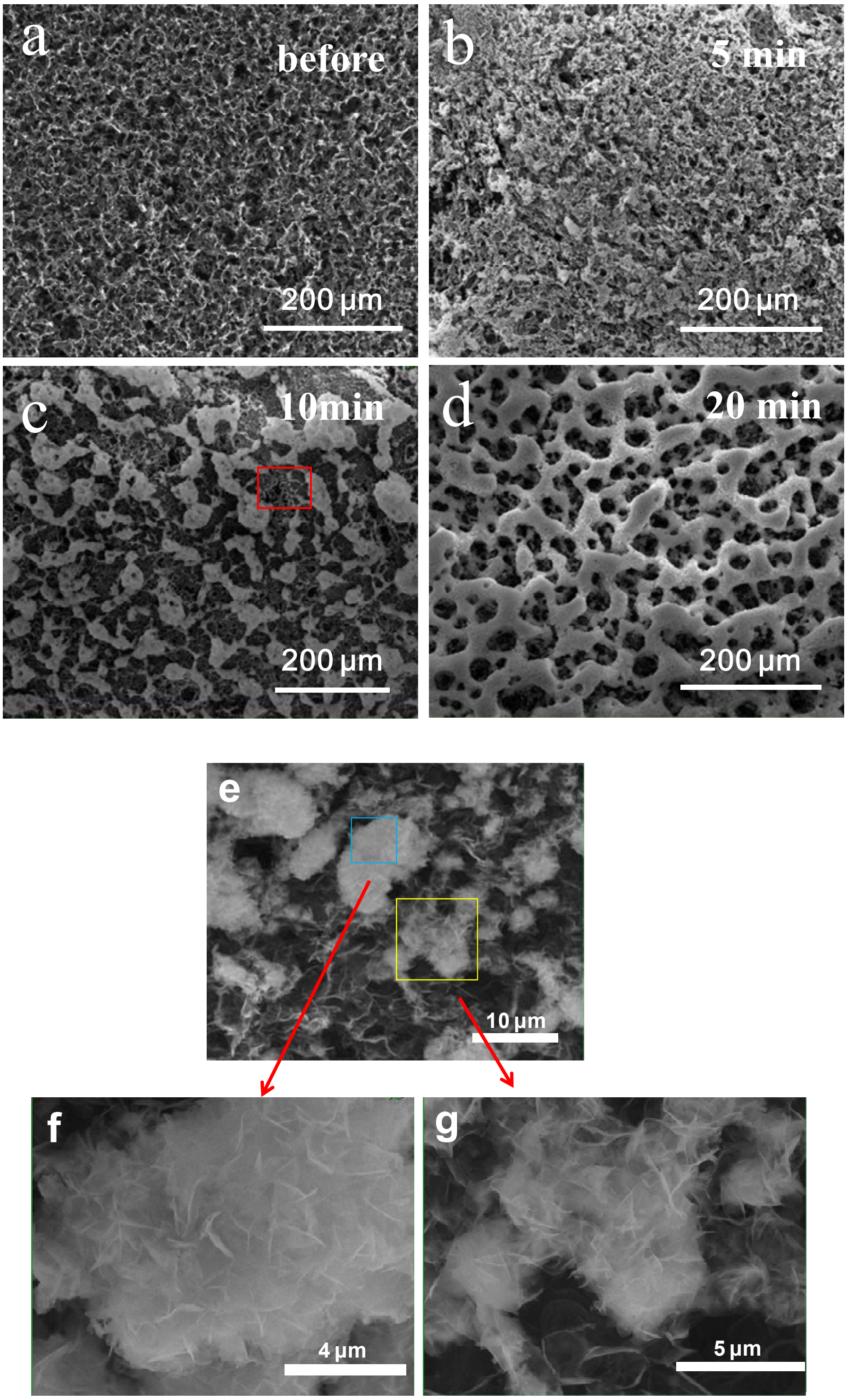

Supplementary Figure S3 | SEM images of 3D-GMOs before and after electrolytic deposition removing Cd^{2+}. (**a**) SEM image of the as-prepared 3D-GMOs.

SEM images of 3D-GMOs after electrolytic deposition removing Cd^{2+} for (**b**) 5 min, (**c**) 10 min and (**d**) 20 min, respectively. (**e**) SEM images of 3D-GMOs after electrolytic deposition removing Cd^{2+} for 10 min in the red rectangle area of Figure **c.** (**f**, **g**) Magnified SEM images of the blue rectangle area and yellow rectangle area in Figure **e,** respectively, which show the graphene layers of 3D-GMOs covered with thin layers of deposited products.

Initially, the honeycomb-like 3D-GMOs provide the large-area templates for deposition. At the beginning, the graphene layers are covered by the thin layer of deposited products. With the deposition time increasing, the covered layer of the deposited products become thicker to form 3D porous layers, which continuously offers the 3D porous template for the subsequent electrolytic deposition.

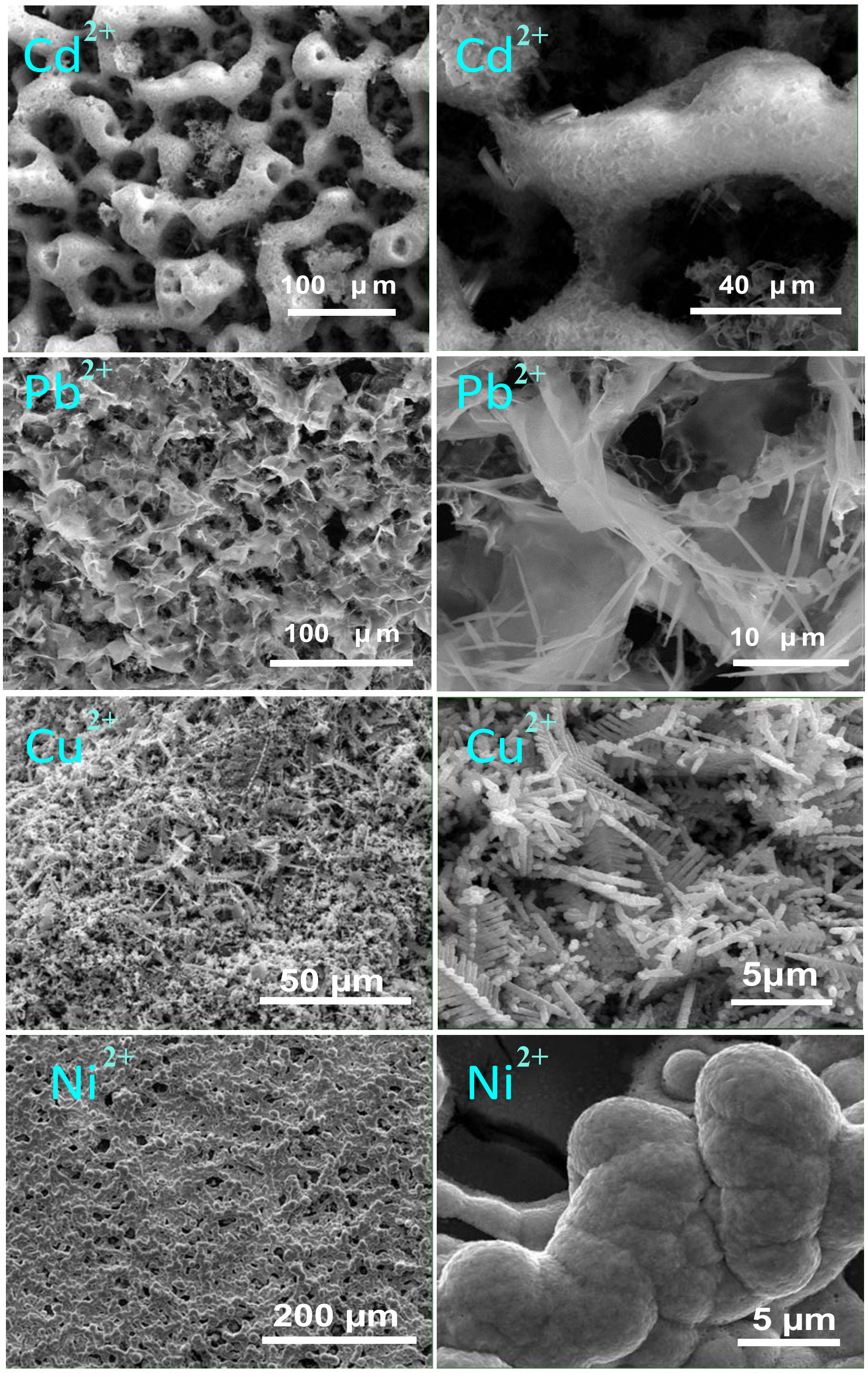

Supplementary Figure S4 | SEM images of 3D-GMOs after electrolytic deposition removing heavy metals ions. SEM images with different magnifications of the electrolytically deposited products of Cd^{2+}, Pb^{2+}, Cu^{2+} and Ni^{2+} (from top to down) on 3D-GMOs for 20 min, respectively. The products deposited on 3D-GMOs show 3D porous structures.

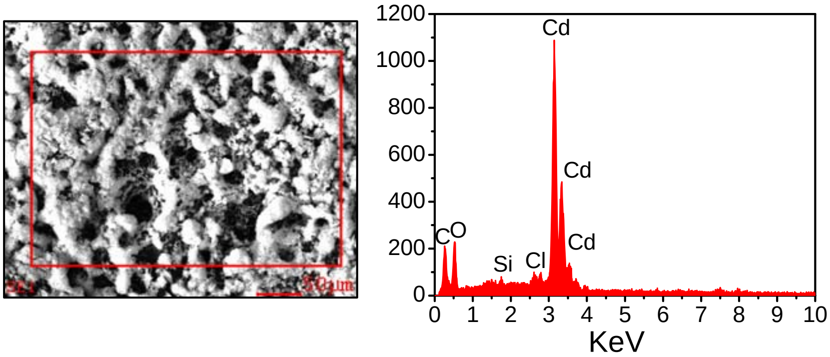

Element	*Wt%*	*At%*
CK	09.01	27.79
OK	20.86	48.29
ClK	01.14	01.19
CdL	68.98	22.73

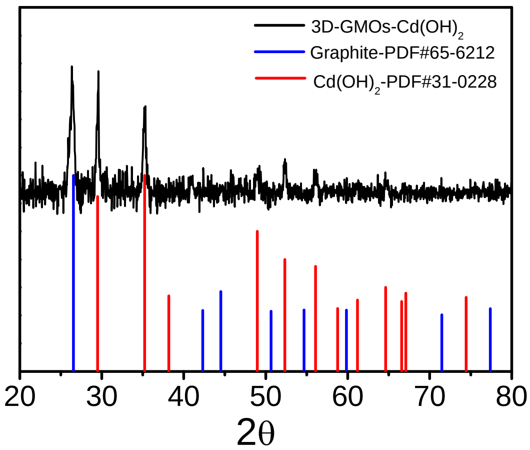

Supplementary Figure S5 | EDX spectrum (up) and XRD pattern (down) of the deposited product of Cd^{2+} for 20min. EDX shows that elements of the selected area are mainly C, O, Cd and Cl, respectively, and the proportions of the elements are list in the upper right table. XRD pattern further confirms that the main product deposited on the 3D-GMO is $Cd(OH)_2$.

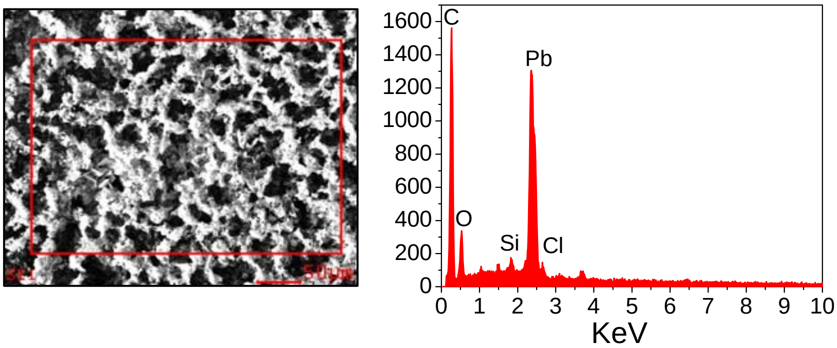

Element	*Wt%*	*At%*
CK	43.54	79.16
OK	11.70	15.97
SiK	00.22	00.17
PbM	44.54	04.70

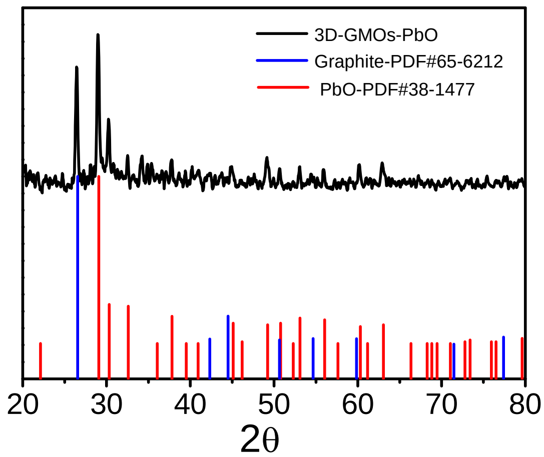

Supplementary Figure S6 | EDX spectrum (up) and XRD pattern (down) of the deposited product of Pb^{2+} for 20min. EDX shows that elements of the selected area are mainly C, O, Pb, respectively, and the proportions of the elements are list in the upper right table. XRD pattern further confirms that the main product deposited on 3D-GMO is PbO.

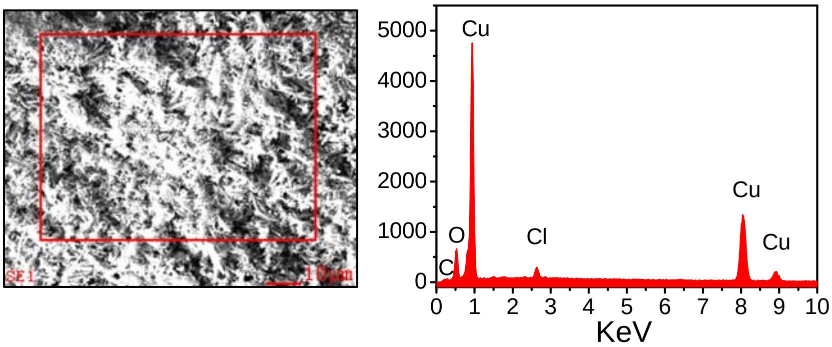

Element	*Wt%*	*At%*
CK	01.59	06.13
OK	09.65	27.90
ClK	02.31	03.02
CuK	86.45	62.96

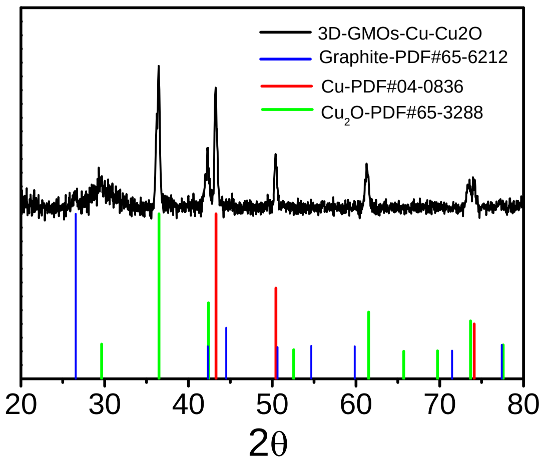

Supplementary Figure S7 | EDX spectrum (up) and XRD pattern (down) of the deposited product of Cu^{2+} for 20min. EDX shows that elements of the selected area are mainly C, O, Cu and Cl, respectively, and the proportions of the elements are list in the upper right table. XRD pattern further confirms that the main products deposited on 3D-GMO are the mixture of Cu_2O and Cu.

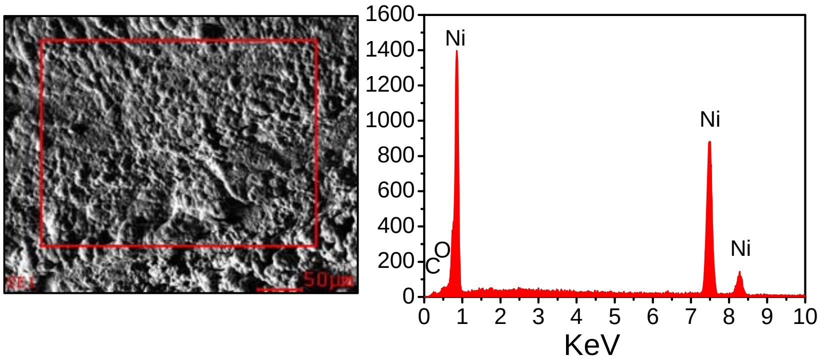

Element	*Wt%*	*At%*
CK	01.19	05.34
OK	01.46	04.94
NiK	97.35	89.71

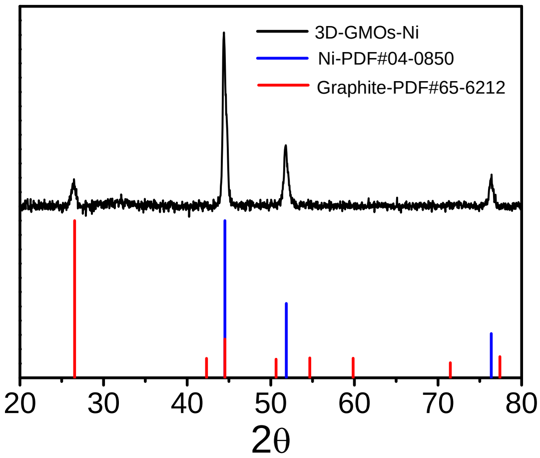

Supplementary Figure S8 | EDX spectrum (up) and XRD pattern (down) of the deposited product of Ni^{2+} for 20min. EDX shows that elements of the selected area are dominantly Ni and a small amount of C and O, respectively, and the proportions of the elements are list in the upper right table. XRD pattern further confirms that the product deposited on the 3D-GMO is Ni metal.

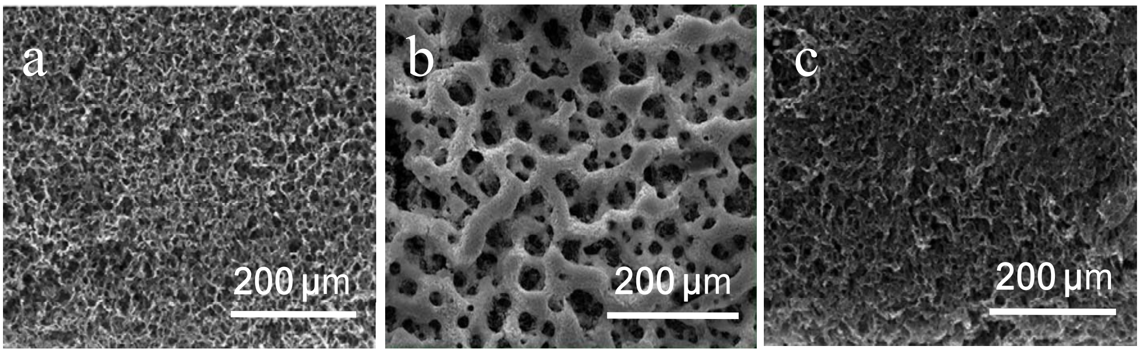

Supplementary Figure S9 | The recovery performance of the deposited products of Cd^{2+} on 3D-GMOs. SEM images of 3D-GMOs before (**a**) and after electrolytic deposition removing Cd^{2+} for 20 min (**b**) followed by the desorption process for 1 min (**c**). Compared with Figure b, the 3D deposited product almost disappeared in Figure c(a desorption efficiency >96%).

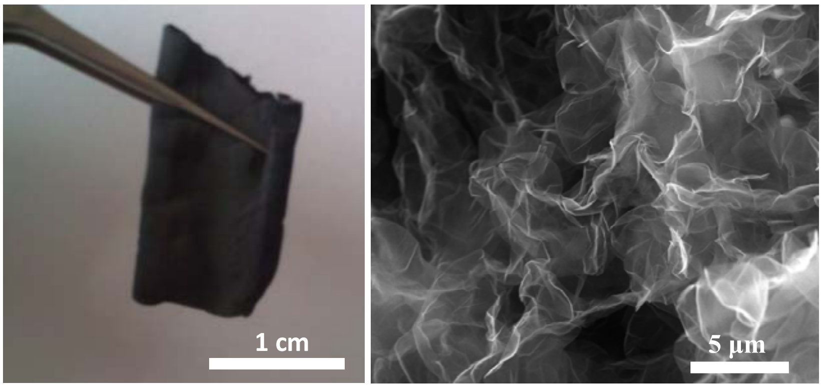

Supplementary Figure S10 | The morphology characterization of 3D-GMOs preparation by using the recycled $NiCl_2$/HCl as the catalyst precursor. Optical image (left) and SEM (right) image of 3D-GMOs after etching the recycled Ni templates by 3M HCl solution. The morphology of the 3D-GMOs grown on the recycled Ni templates is in accordance with that grown on the fresh Ni templates.

Table S1 | Maximum adsorption capacity of related heavy metal ions on graphene based absorbents.

Adsorbents	Heavy Metal ions	Adsorbtion Capacitiy (mg/g)	Reference
EDTA-Graphene Oxide	Pb^{2+}	479 ± 46	1
Graphene–c-MWCNT hybrid aerogel	Pb^{2+} Cu^{2+}	104.9 33.8	2
Few-Layered Graphene Oxide Nanosheets	Cd^{2+}	106.3	3
Folding/aggregation of graphene oxide	Cu^{2+}	46.6	4
Ordered porous chitosan–gelatin/graphene oxide monoliths	Pb^{2+} Cu^{2+}	99 130	5
Polydopamine-Functionalized Graphene Hydrogel	Pb^{2+} Cd^{2}	336.32 145.48	6
Functionalized graphene	Pb^{2+} Cd^{2}	406.6 73.42	7
3D graphene/R-FeOOH hydrogel	Pb^{2+}	373.8	8
Low-Temperature Exfoliated Graphene Nanosheets	Pb^{2+}	40	9
Few-layered graphene oxide 2- or 3-layered graphene	Pb^{2+}	842 (293K) 1150 (313K) 1850 (333K) 400	10
Flower-like TiO_2-graphene oxide	Pb^{2+} Cd^{2+}	65.6± 2.7 72.8±1.6	11
GO/Fe_3O_4	Cu^{2+}	18.26 (293K)	12
3D-GMOs	Pb^{2+} Cd^{2+} Cu^{2+} Ni^{2+}	882 434 3820 1683	This work
GNS/δ-MnO2	Ni^{2+}	46.55	13

References

1. Madadrang C. J. *et al*. Adsorption behavior of EDTA-graphene oxide for Pb (II) removal. *ACS Appl. Mater. Interfaces* **4**, 1186-1193 (2012).
2. Sui, Z. Y., Meng, Q. H, Zhang, X. T, Ma, R. & Cao, B. Green synthesis of carbon nanotube-graphene hybrid aerogels and their use as versatile agents for water purification. *J. Mater. Chem.* **22**, 8767-8771 (2012).
3. Zhao, G. X., Li, J. X., Ren, X. M., Chen, C. L. & Wang, X. K. Few-layered graphene oxide nanosheets as superior sorbents for heavy metal ion pollution management. *Environ. Sci. Technol.* **45**, 10454-10462 (2011).
4. Yang, S. T. *et al*. Folding/aggregation of graphene oxide and its application in Cu^{2+} removal. *J. Colloid Interface Sci.* **351**, 122-127 (2010).
5. Zhang, N. N, Qiu, H. X., Si, Y. M., Wang, W. & Gao, J. P. Fabrication of highly porous biodegradable monoliths strengthened by graphene oxide and their adsorption of metal ions. *Carbon* **49**, 827-837 (2011).
6. Gao, H. C., Sun, Y. M., Zhou, J. J., Xu, R. & Duan, H.W. Mussel-inspired synthesis of polydopamine-functionalized graphene hydrogel as reusable adsorbents for water purification. *ACS Appl. Mater. Interfaces* **5**, 425-432 (2013).
7. Deng, X. J., Lu, L. L., Li, H. W. & Luo, F. The adsorption properties of Pb (II) and Cd (II) on functionalized graphene prepared by electrolysis method. *J. Hazard. Mater.* **183**, 923-930 (2010).

8. Cong, H. P., Ren, X. C., Wang, P. & Yu, S. H. Macroscopic multifunctional graphene-based hydrogels and aerogels by a metal ion induced self-assembly process. *ACS Nano* **6**, 2693-2703 (2012).

9. Huang, Z. H. *et al*. Adsorption of lead (II) ions from aqueous solution on low-temperature exfoliated graphene nanosheets. *Langmuir* **27**, 7558-7562 (2011).

10. Zhao. G. X. *et al*. Removal of Pb (II) ions from aqueous solutions on few-layered graphene oxide nanosheets. *Dalton Trans.* **40**, 10945–10952 (2011).

11. Lee, Y. C. & Yang, J. W. Self-assembled flower-like TiO_2 on exfoliated graphite oxide for heavy metal removal. *J. Ind. and Eng. Chem.* **18**, 1178-1185 (2012).

12. Li, J. *et al*. Removal of Cu (II) and fulvic acid by graphene oxide nanosheets decorated with Fe_3O_4 nanoparticles. *ACS Appl. Mater. Interfaces* **4**, 4991-5000 (2012).

13. Ren, Y. M. *et al*. Graphene/δ-MnO_2 composite as adsorbent for the removal of nickel ions from wastewater. *Chem. Eng. J.* **175**, 1-7 (2011).